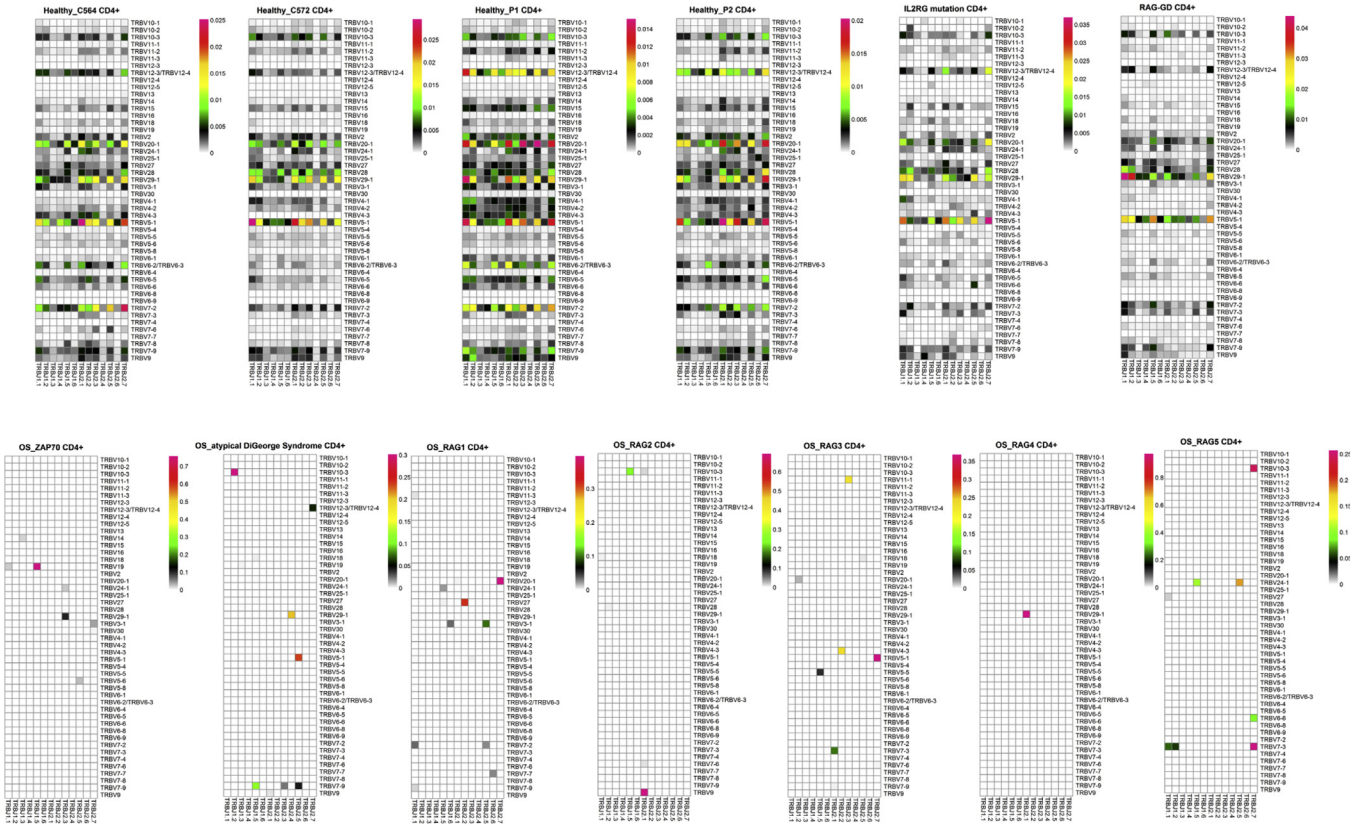

FIG E1. Two-dimensional heat maps of TCRβ V-J use for $CD4^+$ T cells from each subjects. The different Vβ genes are on the longitudinal ordinate, and the different Jβ genes are on the horizontal ordinate.

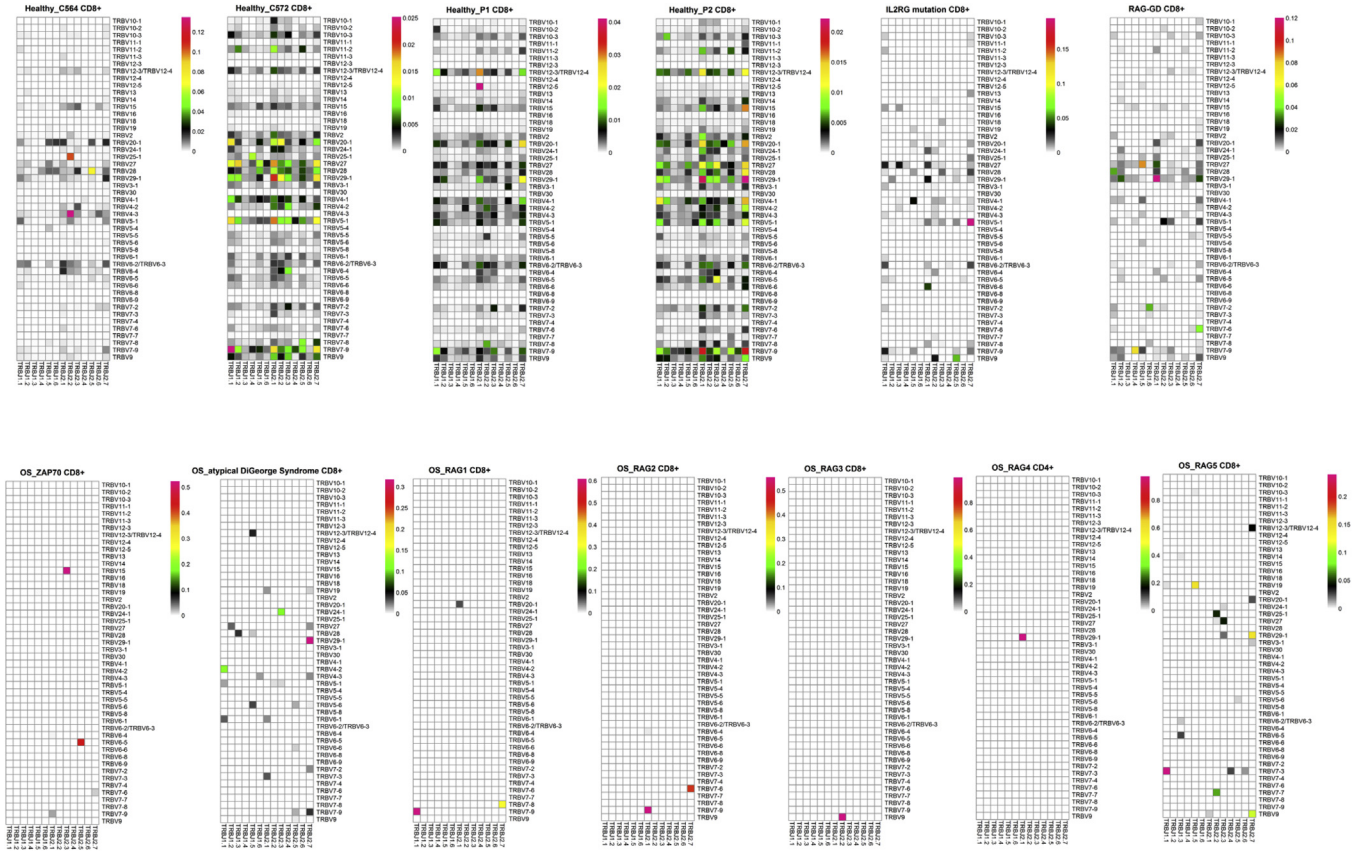

FIG E2. Two-dimensional heat maps of TCRβ V-J use for $CD8^+$ T cells from each subject. The different Vβ genes are on the longitudinal ordinate, and the different Jβ genes are on the horizontal ordinate.

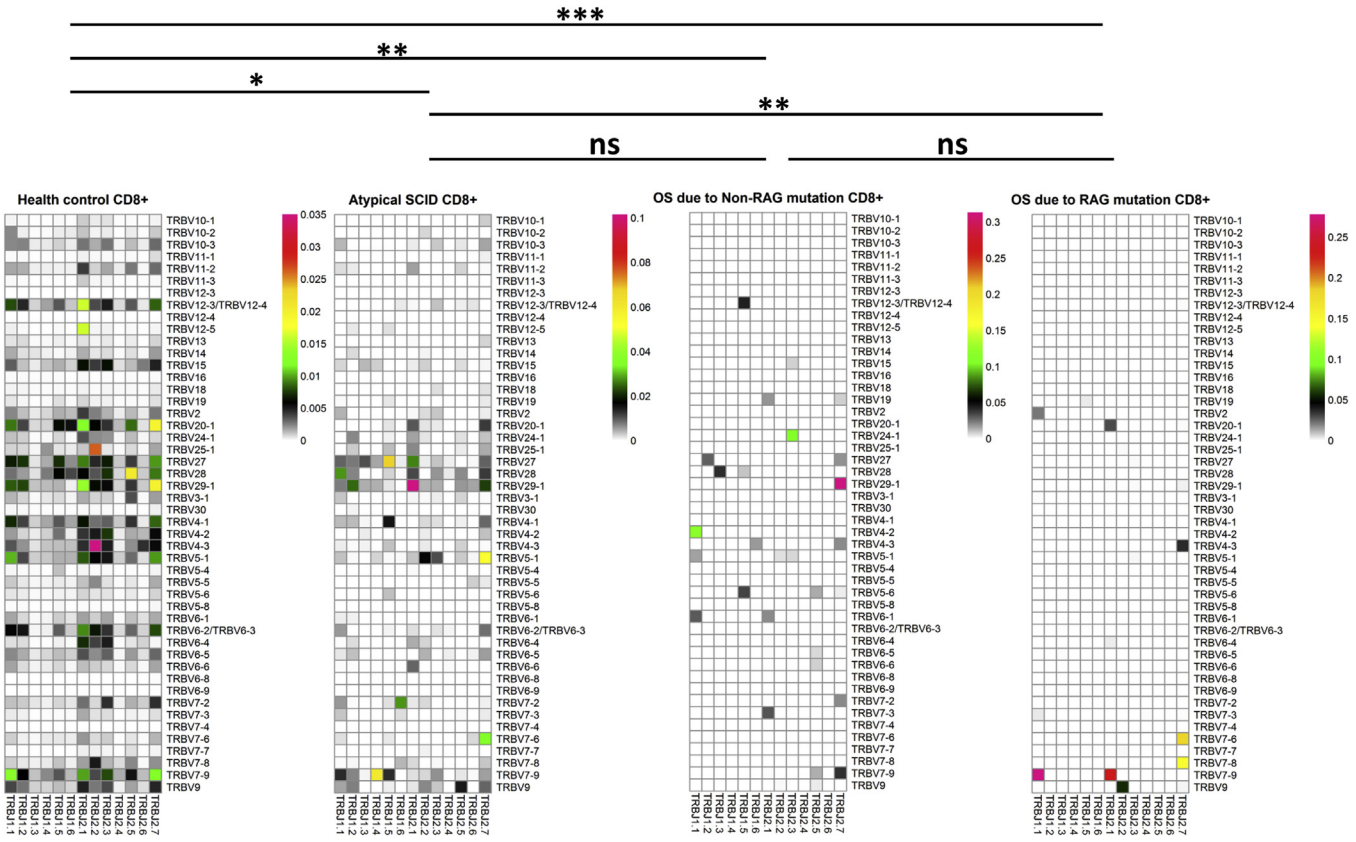

FIG E3. Two-dimensional heat maps of TCRβ V-J use for $CD8^+$ T cells from healthy control subjects, patients with atypical SCID (*IL2RG* mutation and granulomatous disease caused by *RAG* mutation—RAG granulomatous disease), patients with OS caused by non-*RAG* mutations, and patients with OS caused by *RAG* mutations. The different Vβ genes are on the longitudinal ordinate, and the different Jβ genes are on the horizontal ordinate. *P* values of unpaired *t* tests are shown: *.01 < *P* < .05, **.001 < *P* < .01, and ***$P < .001$. *ns*, Nonsignificant.

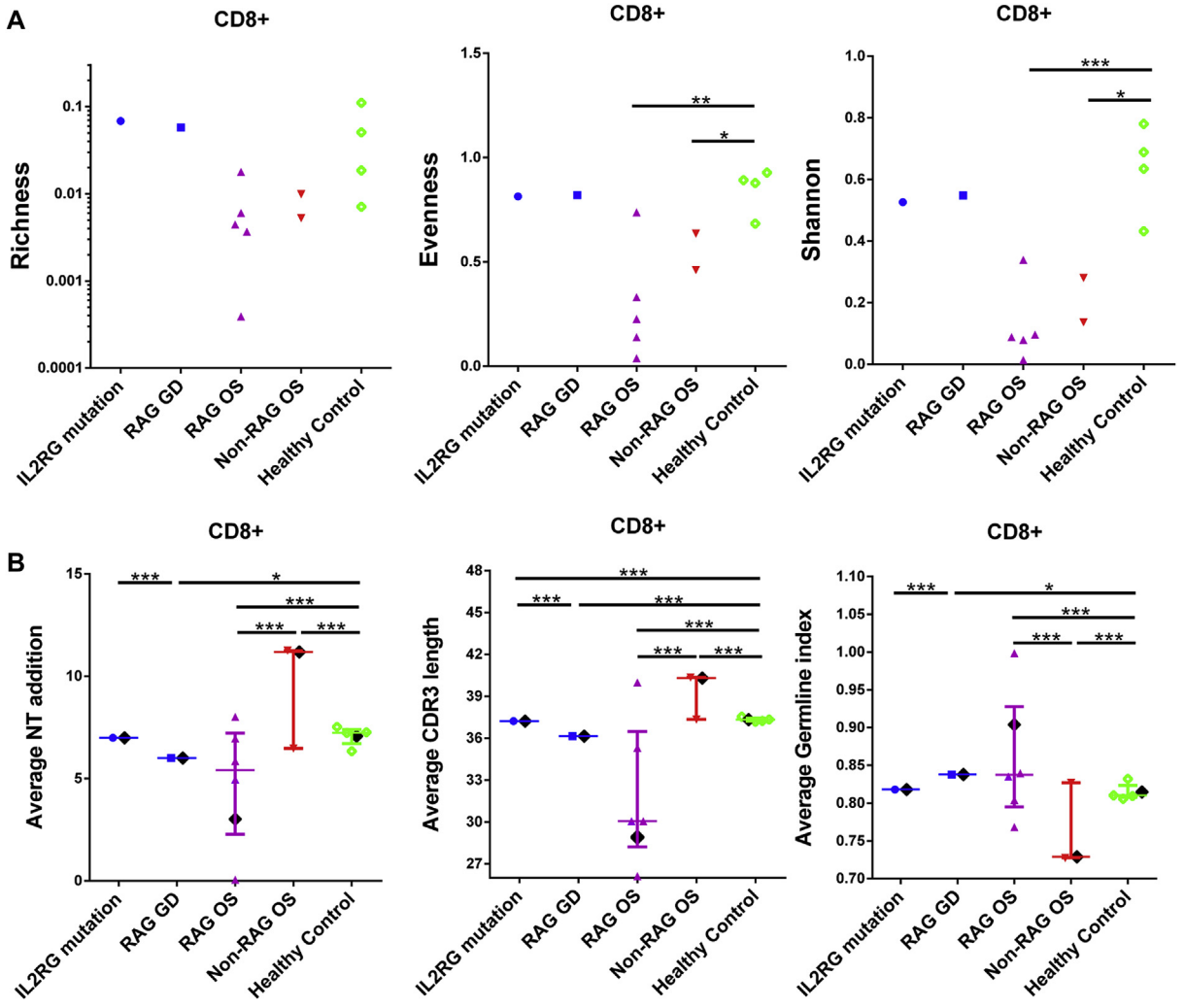

FIG E4. Repertoire characteristics of $CD8^+$ T cells from patients and healthy control subjects. Richness, evenness, and Shannon entropy **(A)** and junctional nucleotide additions, CDR3 length, and germline index **(B)** were calculated for total annotated TCRβ sequence reads from individual patients, as well as total annotated TCRβ sequence reads from all subjects in same group, and compared with each other. Patients with atypical SCID, patients with OS caused by *RAG* mutations *(RAG OS)*, patients with OS caused by non-*RAG* mutations *(Non-RAG OS)*, and healthy control subjects are shown in *blue, purple, red,* and *green,* respectively. The *black diamond* represents the mean value calculated from pooled TCRβ sequences from all subjects of the same group. Medians with interquartile ranges are shown in each group. *P* values of unpaired *t* tests are shown as follows: *.01 < *P* < .05, **.001 < *P* < .01, and ***P < .001.

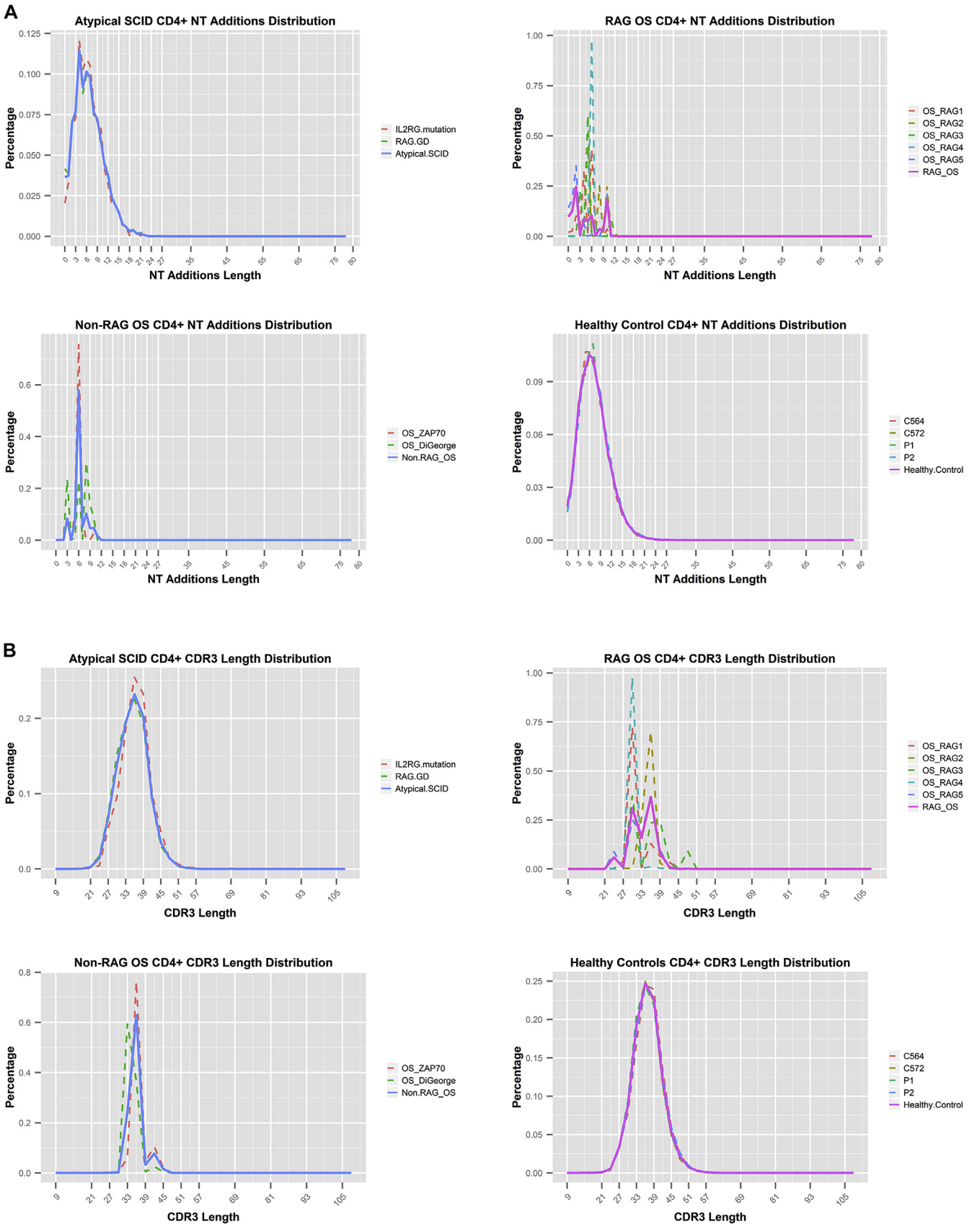

FIG E5. A, Nucleotide *(NT)* additions in junctional regions of CDR3 for all unique $CD4^+$ T-cell TCRβ sequences from patients with atypical SCID, patients with OS caused by *RAG* mutations, patients with OS caused by non-*RAG* mutations, and healthy control subjects. **B,** CDR3 length distribution of all unique $CD4^+$ T-cell TCRβ sequences from patients with atypical SCID, patients with OS caused by *RAG* mutations, patients with OS caused by non-*RAG* mutations, and healthy control subjects.

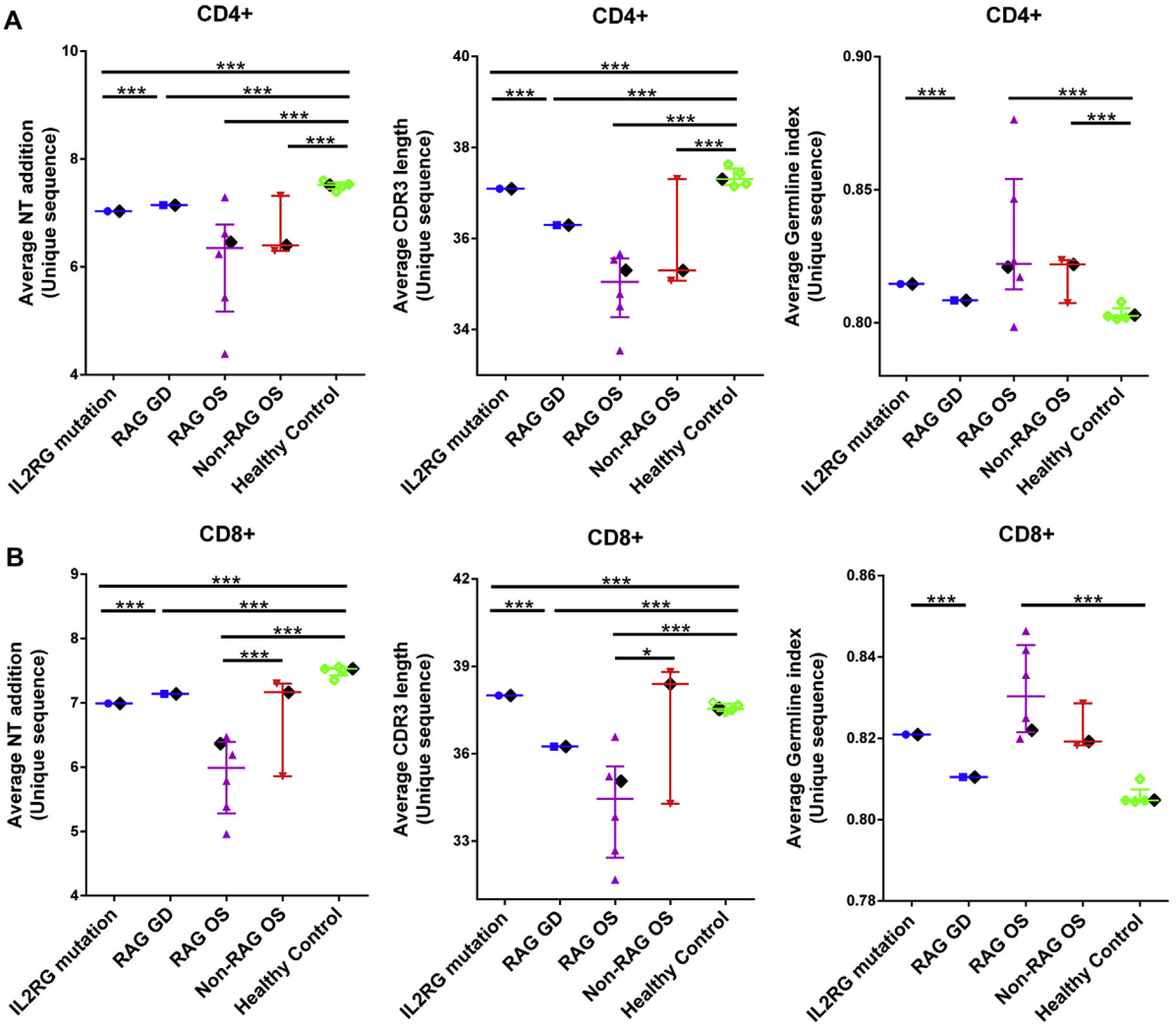

FIG E6. Repertoire characteristics of unique $CD4^+$ and $CD8^+$ TCRβ sequences from patients and healthy control subjects. **A,** Junctional nucleotide additions, CDR3 length, and germline index were calculated for unique $CD4^+$ annotated TCRβ sequence reads from individual patients, as well as unique $CD4^+$ annotated TCRβ sequence reads from all subjects in same group, and compared with each other. **B,** Junctional nucleotide additions, CDR3 length, and germline index were calculated for unique $CD8^+$ annotated TCRβ sequence reads from individual patients, as well as unique $CD8^+$ annotated TCRβ sequence reads from all subjects in the same group, and compared with each other. Patients with atypical SCID, patients with OS caused by *RAG* mutations, patients with OS caused by non-*RAG* mutations, and healthy control subjects are shown in *blue, purple, red,* and *green,* respectively. The *black diamond* represents the mean value calculated from pooled TCRβ sequences from all subjects of the same group. Medians with interquartile ranges are shown in each group. *P* values of unpaired *t* tests are shown as follows: *.01 < *P* < .05, **.001 < *P* < .01, and ***P < .001.

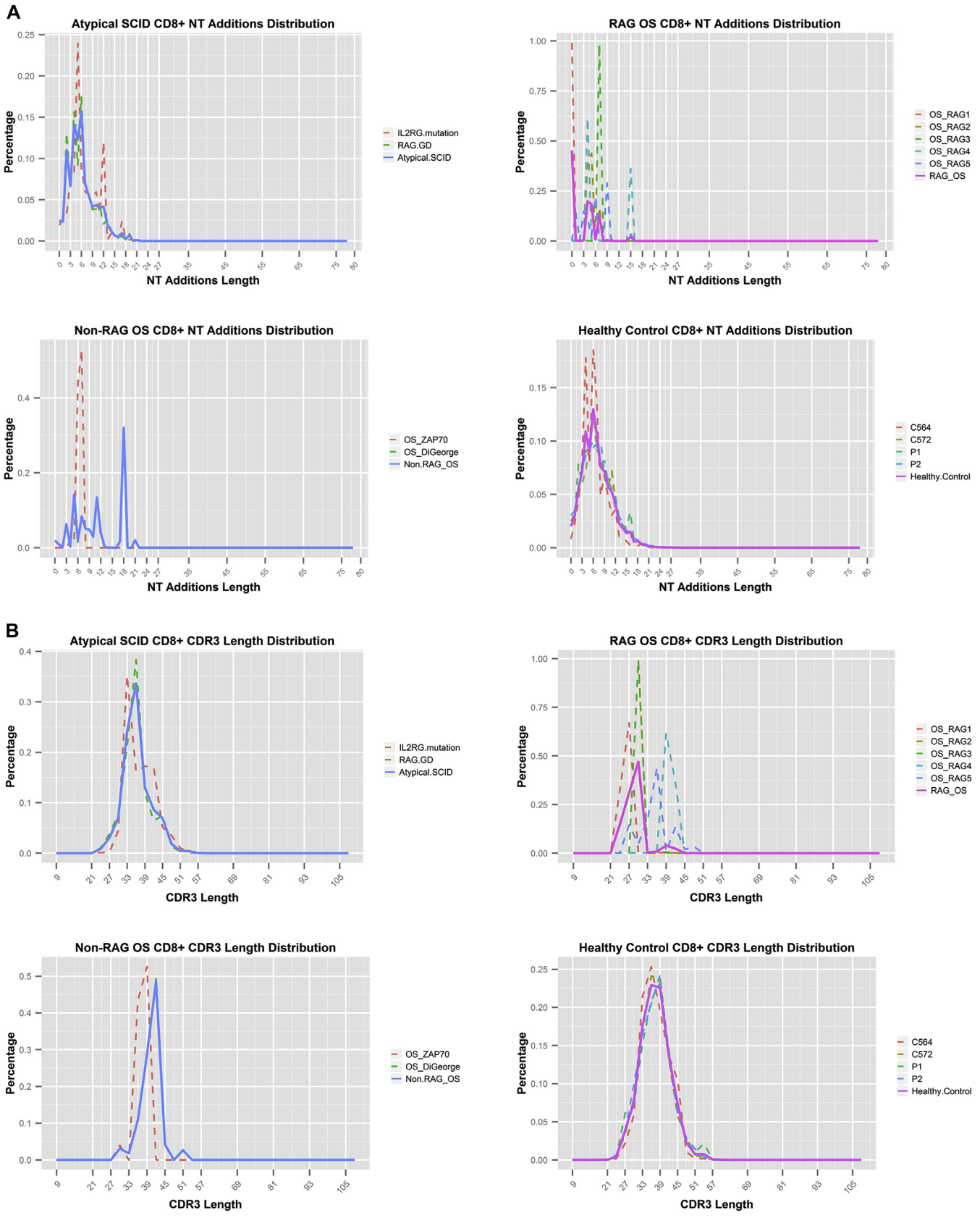

FIG E7. A, Nucleotide *(NT)* additions in junctional regions of CDR3 for all unique $CD8^+$ T-cell TCRβ sequences from patients with atypical SCID, patients with OS caused by *RAG* mutations, patients with OS caused by non-*RAG* mutations, and healthy control subjects. **B,** CDR3 length distribution of all unique $CD8^+$ T-cell TCRβ sequences from patients with atypical SCID, patients with OS caused by *RAG* mutations, patients with OS caused by non-*RAG* mutations, and healthy control subjects.

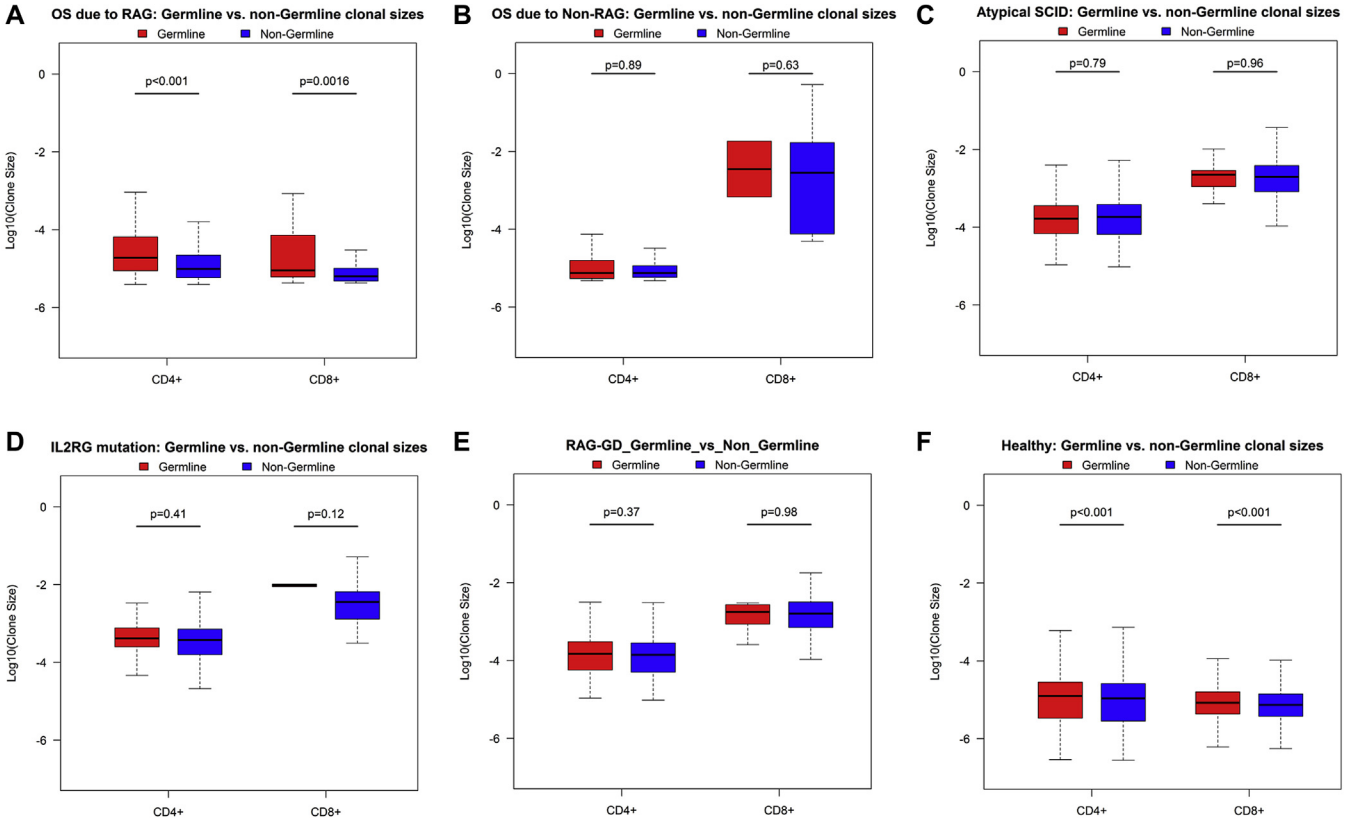

FIG E8. A, *Box plots* show that the clone size of $CD4^+$ and $CD8^+$ T-cell germline sequences is significantly bigger than that of nongermline TCRβ sequences in patients with OS caused by *RAG* mutations. **B,** *Box plots* show that the clone size of $CD4^+$ and $CD8^+$ T-cell germline sequences is slightly bigger than that of nongermline TCRβ sequences in patients with OS caused by non-*RAG* mutations. **C,** *Box plots* show that the clone size of $CD4^+$ T-cell germline sequences is slighter smaller than that of nongermline TCRβ sequences in patients with atypical SCID and the clone size of $CD8^+$ T-cell germline sequences is slightly smaller than that of nongermline TCRβ sequences. **D,** *Box plots* show that the clone size of $CD4^+$ and $CD8^+$ T-cell germline sequences is slightly bigger than that of nongermline TCRβ sequences in patient with *IL2RG* mutations. **E,** *Box plots* show that the clone size of $CD4^+$ and $CD8^+$ T-cell germline sequences is slightly bigger than that of nongermline TCRβ sequences in patients with granulomatous disease caused by *RAG* mutations. **F,** *Box plots* show that the clone size of $CD4^+$ and $CD8^+$ T-cell germline sequences is significantly bigger than that of nongermline TCRβ sequences in healthy control subjects. *P* values of the Wilcoxon rank sum test are shown.

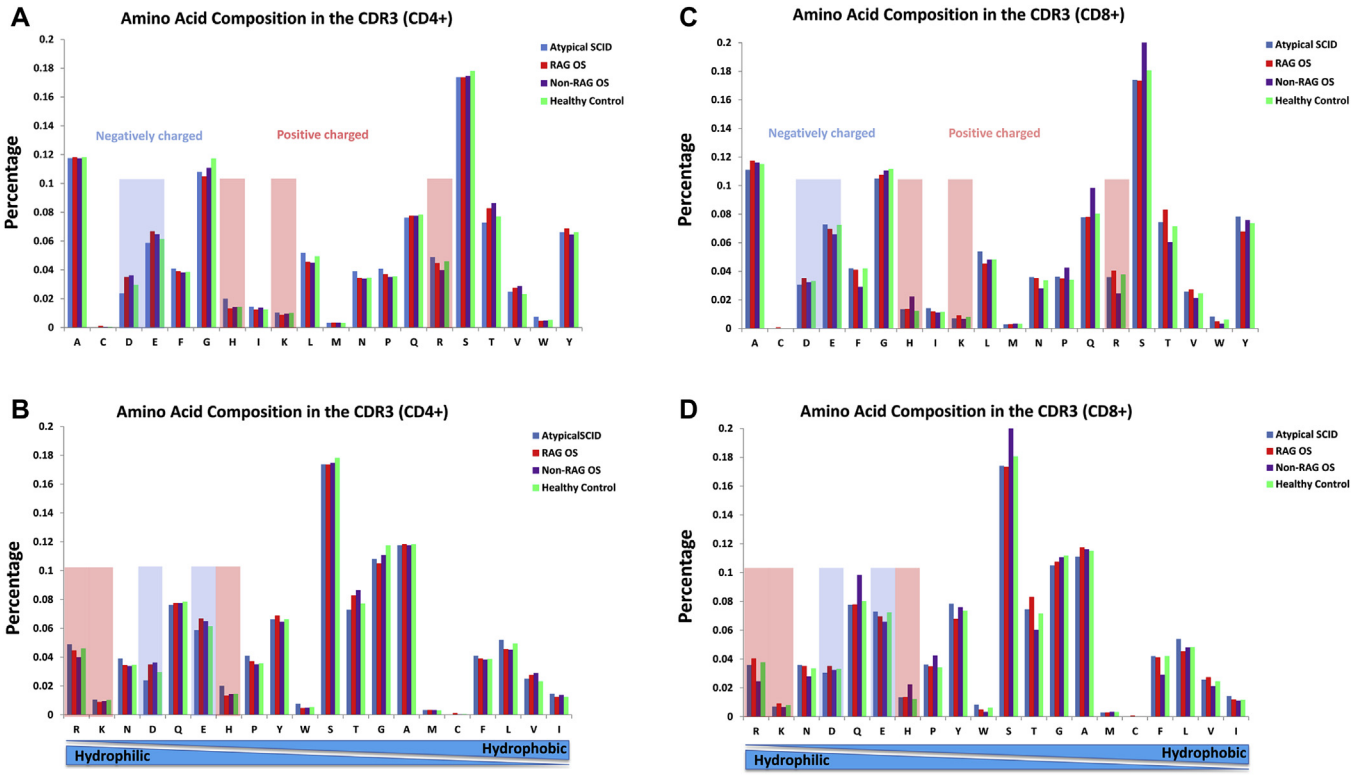

FIG E9. A, Amino acid frequencies of CDR3s for all unique $CD4^+$ T-cell TCRβ sequences from patients with atypical SCID, patients with OS caused by *RAG* mutations, patients with OS caused by non-*RAG* mutations, and healthy control subjects. **B,** Amino acid frequencies of the CDR3s for all unique $CD4^+$ T-cell TCRβ sequences from patients with atypical SCID, patients with OS caused by *RAG* mutations, patients with OS caused by non-*RAG* mutations, and healthy control subjects (amino acids are ranked from hydrophilic to hydrophobic). **C,** Amino acid frequencies of the CDR3s for all unique $CD8^+$ T-cell TCRβ sequences from patients with atypical SCID, patients with OS caused by *RAG* mutations, patients with OS caused by non-*RAG* mutations, and healthy control subjects. **D,** Amino acid frequencies of the CDR3s for all unique $CD8^+$ T-cell TCRβ sequences from patients with atypical SCID, patients with OS caused by *RAG* mutations, patients with OS caused by non-*RAG* mutations, and healthy control subjects (amino acids are ranked from hydrophilic to hydrophobic). Negatively charged amino acids are shown in *light blue*, and positively charged amino acids are shown in *pink*.

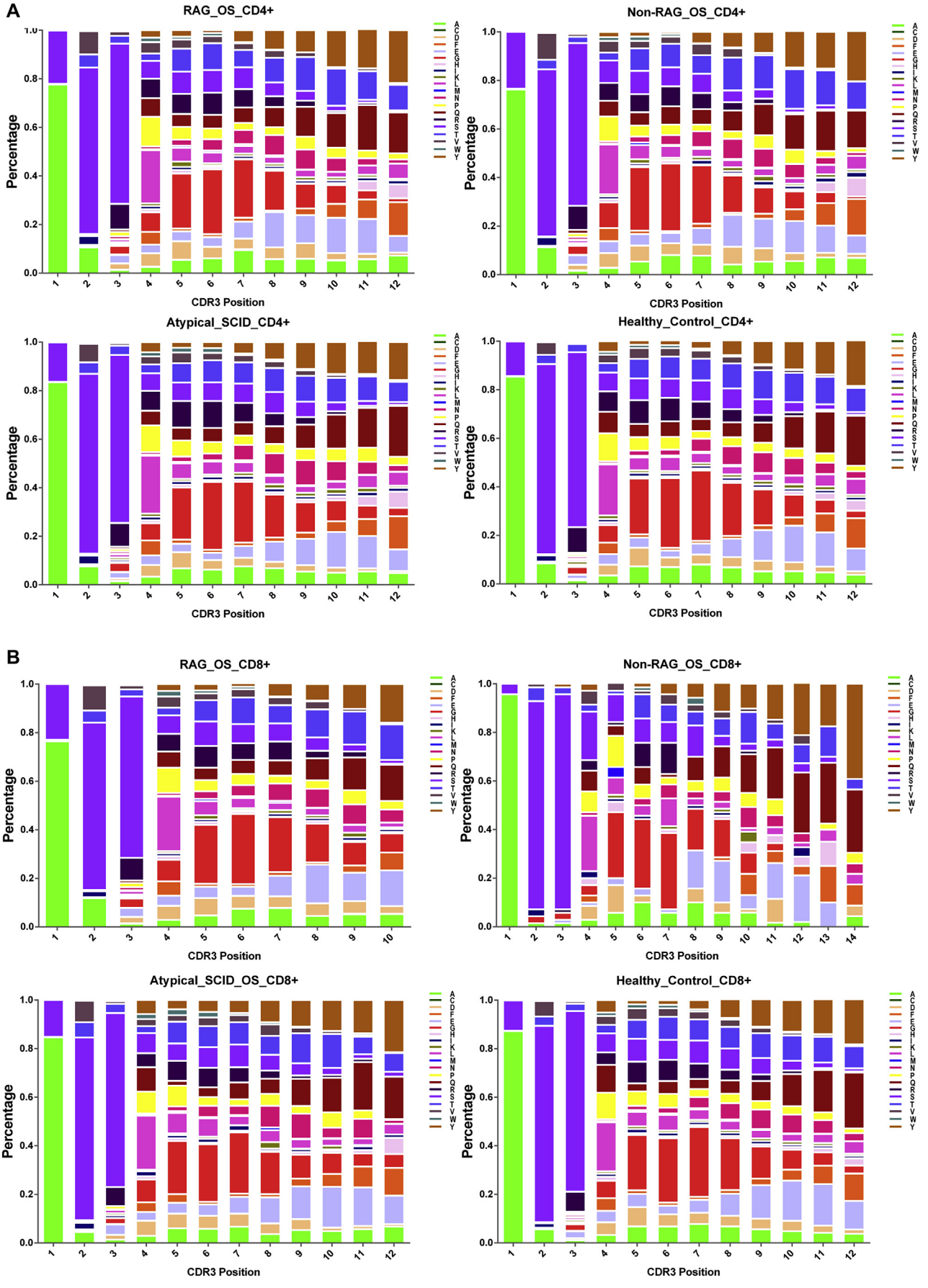
A
RAG_OS_CD4+
Non-RAG_OS_CD4+
Atypical_SCID_CD4+
Healthy_Control_CD4+
Percentage
CDR3 Position
B
RAG_OS_CD8+
Non-RAG_OS_CD8+
Atypical_SCID_OS_CD8+
Healthy_Control_CD8+
Percentage
CDR3 Position

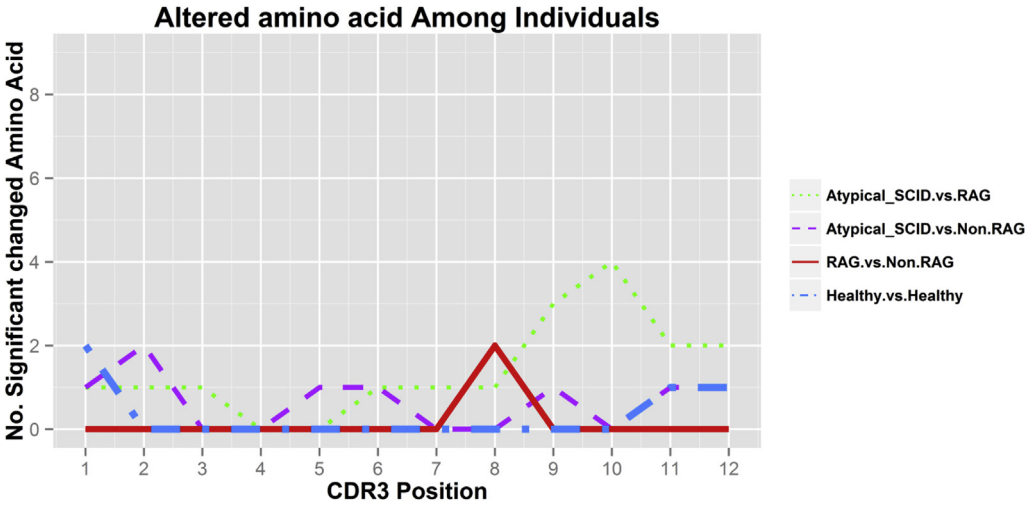

FIG E11. Number of significantly changed amino acids of CDR3s (position 1-36 nt) for all unique $CD4^+$ T-cell annotated TCRβ sequence reads from patients with atypical SCID compared with patients with OS caused by *RAG* mutations, patients with atypical SCID compared with patients with OS caused by non-*RAG* mutations, patients with OS caused by *RAG* mutations compared with patients with OS caused by non-*RAG* mutations, and among the healthy control subjects.

FIG E10. A, Amino acid composition of each position of CDR3s for all unique $CD4^+$ T-cell TCRβ sequences (position 1-36 nt) from patients with OS caused by *RAG* mutations, patients with OS caused by non-*RAG* mutations, patients with atypical SCID, and healthy control subjects. **B,** Amino acid composition of each position of CDR3s for all unique $CD8^+$ T-cell TCRβ sequences from patients with OS caused by *RAG* mutations (position 1-30 nt), patients with OS caused by non-*RAG* mutations (position 1-42 nt), patients with atypical SCID (position 1-36 nt), and healthy control subjects (position 1-36 nt).

TABLE E1. TCRβ sequence statistics*

Group	Subject	Cell type	Cell count	Annotated TCRβ	Coverage	Unique TCRβ
Atypical SCID	CMNL13687†	$CD4^+$	26,657	474,311	17.7931125032824	1,753
	1228601†	$CD4^+$	61,892	1,464,972	23.6698119304595	4,642
RAG OS	OS_RAG1	$CD4^+$	161,500	1,525,164	9.44373993808049	1,668
	OS_RAG2	$CD4^+$	74,300	1,536,225	20.6759757738896	58
	OS_RAG3	$CD4^+$	8,000	178,073	22.259125	35
	OS_RAG4	$CD4^+$	23,400	413,879	17.6871367521367	244
	OS_RAG5	$CD4^+$	53,000	7,244,060	136.68037735849	110
Non-RAG OS	DIG†	$CD4^+$	18,600	1,498,867	80.5842473118279	84
	PB7†	$CD4^+$ memory	126,000	2,931,851	23.2686587301587	754
Healthy control	C564	$CD4^+$	1,000,000	48,861,777	48.861777	27,849
	C572	$CD4^+$	2,000,000	117,240,980	58.62049	39,916
	P1	$CD4^+$	1,000,000	29,620,188	29.620188	76,431
	P2	$CD4^+$	1,000,000	57,487,033	57.487033	53,072
Atypical SCID	CMNL13687	$CD8^+$	1,973	44,655	22.6330461226558	134
	1228601	$CD8^+$	5,417	166,476	30.7321395606424	305
RAG OS	OS_RAG1	$CD8^+$	146,100	1,870,717	12.8043600273785	877
	OS_RAG2	$CD8^+$	64,000	1,697,549	26.524203125	24
	OS_RAG3	$CD8^+$	6,300	233,789	37.109365079365	28
	OS_RAG4	$CD8^+$	9,800	240,207	24.5109183673469	34
	OS_RAG5	$CD8^+$	1,740	53,734	30.8816091954022	30
Non-RAG OS	DIG	$CD8^+$	12,000	2,263,323	188.61025	59
	PB7	$CD8^+$	708	33,106	46.7598870056497	6
Healthy control	C564	$CD8^+$	700,000	25,522,565	36.4608071428571	4,835
	C572	$CD8^+$	1,000,000	25,989,097	25.989097	17,333
	P1	$CD8^+$	1,000,000	24,868,092	24.868092	50,395
	P2	$CD8^+$	1,000,000	17,265,532	17.265532	109,599

**Annotated TCRβ*, Total sequences in which TCRβ V, D, and J genes could be identified; *Cell count*, cells were counted after sorting; *Coverage*, coverage is calculated as the total count of annotated reads/cell count used for library generation; *Unique TCRβ*, number of each TCRβ species.

†CMNL13687 is a patient with the *IL2RG* mutation, 1228601 is a patient with granulomatous disease caused by a *RAG* mutation, DIG is a patient with OS caused by atypical complete DiGeorge syndrome, and PB7 is a patient with OS caused by *ZAP70* mutation.

TABLE E2. Healthy control subjects and patients studied according to the clinical group with the list of mutations

	Lymphocytosis	Erythroderma, high IgE level	SCID-related infections	Autoimmunity	Granulomas
Healthy control subjects	No	No	No	No	No
OS caused by *RAG* mutations (n = 5)	Yes	Yes	Yes	No	No
OS caused by *ZAP70* mutations	Yes	Yes	Yes	No	No
OS caused by atypical complete DiGeorge syndrome	Yes	Yes	Yes	No	No
Granulomatous disease caused by *RAG* mutations	No	No	Mild	Yes	No
IL2RG mutation	No	No	Delayed, mild	Yes	Yes

TABLE E3. Primers used in amplifying TCRβ

Name	Code	Sequence	Information
5PIIA		**AAGCAGTGGTATCAACGCAGAGT**	First PCR: F
PE1 FCB ILL 1_2 V2	162448A01	AATGATACGGCGACCACCGAGA**TCT**ACACTCTTTCCCTA*CACGACGCTCTTCCGATCT*	Second PCR: F1
PE1 ILL BC 5PIIA 2_2 1	162820E06	*CACGACGCTCTTCCGATCT*NN CGTGAT **AAGCAGTGGTATCAACGCAGAGT**	BC 01: F2
PE1 ILL BC 5PIIA 2_2 2	162820E12	*CACGACGCTCTTCCGATCT*NNN ACATCG **AAGCAGTGGTATCAACGCAGAGT**	BC 02: F2
PE1 ILL BC 5PIIA 2_2 3	162820F07	*CACGACGCTCTTCCGATCT*NNNN GCCTAA **AAGCAGTGGTATCAACGCAGAGT**	BC 03: F2
PE1 ILL BC 5PIIA 2_2 4	162820E07	*CACGACGCTCTTCCGATCT*NN TGGTCA **AAGCAGTGGTATCAACGCAGAGT**	BC 04: F2
PE1 ILL BC 5PIIA 2_2 5	162820F01	*CACGACGCTCTTCCGATCT*NNN CACTGT **AAGCAGTGGTATCAACGCAGAGT**	BC 05: F2
PE1 ILL BC 5PIIA 2_2 6	162820F08	*CACGACGCTCTTCCGATCT*NNNN ATTGGC **AAGCAGTGGTATCAACGCAGAGT**	BC 06: F2
PE1 ILL BC 5PIIA 2_2 7	162820E08	*CACGACGCTCTTCCGATCT*NN GATCTG **AAGCAGTGGTATCAACGCAGAGT**	BC 07: F2
PE1 ILL BC 5PIIA 2_2 8	162820F02	*CACGACGCTCTTCCGATCT*NNN TCAAGT **AAGCAGTGGTATCAACGCAGAGT**	BC 08: F2
PE1 ILL BC 5PIIA 2_2 9	162820F09	*CACGACGCTCTTCCGATCT*NNNN CTGATC **AAGCAGTGGTATCAACGCAGAGT**	BC 09: F2
PE1 ILL BC 5PIIA 2_2 10	162820E11	*CACGACGCTCTTCCGATCT*NN AAGCTA **AAGCAGTGGTATCAACGCAGAGT**	BC 10: F2
PE1 ILL BC 5PIIA 2_2 11	162820F03	*CACGACGCTCTTCCGATCT*NNN GTAGCC **AAGCAGTGGTATCAACGCAGAGT**	BC 11: F2
PE1 ILL BC 5PIIA 2_2 12	162820F10	*CACGACGCTCTTCCGATCT*NNNN TACAAG **AAGCAGTGGTATCAACGCAGAGT**	BC 12: F2
PE1 ILL BC 5PIIA 2_2 13	162820E10	*CACGACGCTCTTCCGATCT*NN TTGACT **AAGCAGTGGTATCAACGCAGAGT**	BC 13: F2
PE1 ILL BC 5PIIA 2_2 14	162820F04	*CACGACGCTCTTCCGATCT*NNN GGAACT **AAGCAGTGGTATCAACGCAGAGT**	BC 14: F2
PE1 ILL BC 5PIIA 2_2 15	162820F11	*CACGACGCTCTTCCGATCT*NNNN TGACAT **AAGCAGTGGTATCAACGCAGAGT**	BC 15: F2
PE1 ILL BC 5PIIA 2_2 16	162820E05	*CACGACGCTCTTCCGATCT*NN GGACGG **AAGCAGTGGTATCAACGCAGAGT**	BC 16: F2
PE1 ILL BC 5PIIA 2_2 17	162820F05	*CACGACGCTCTTCCGATCT*NNN CTCTAC **AAGCAGTGGTATCAACGCAGAGT**	BC 17: F2
PE1 ILL BC 5PIIA 2_2 18	162820F12	*CACGACGCTCTTCCGATCT*NNNN GCGGAC **AAGCAGTGGTATCAACGCAGAGT**	BC 18: F2
PE1 ILL BC 5PIIA 2_2 19	162820E09	*CACGACGCTCTTCCGATCT*NN TTTCAC **AAGCAGTGGTATCAACGCAGAGT**	BC 19: F2
PE1 ILL BC 5PIIA 2_2 20	162820G01	*CACGACGCTCTTCCGATCT*NNNN GGCCAC **AAGCAGTGGTATCAACGCAGAGT**	BC 20: F2
HS RJ1_1	162820C04	TTCAGGTCCTCTACAACTGTGAGTCTGGTGCC	Human read 2 primer
HS RJ1_2	162820C05	TTCAGGTCCTCTACAACGGTTAACCTGGTCCC	Human read 2 primer
HS RJ1_3	162820C02	TTCAGGTCCTCTACAACAGTGAGCCAACTTCC	Human read 2 primer
HS RJ1_4	162820D01	TTCAGGTCCTCCAAGACAGAGAGCTGGGTTCC	Human read 2 primer
HS RJ1_5	162820D02	TTCAGGTCCTCTAGGATGGAGAGTCGAGTCCC	Human read 2 primer
HS RJ1_6	162820C08	TTCAGGTCCTCTGTCACAGTGAGCCTGGTCCC	Human read 2 primer
HS RJ2-1	162820C07	TTCAGGTCCTCTAGCACGGTGAGCCGTGTCCC	Human read 2 primer
HS RJ2-2	162820C06	TTCAGGTCCTCCAGTACGGTCAGCCTAGAGCC	Human read 2 primer
HS RJ2-3	162820C03	TTCAGGTCCTCGAGCACTGTCAGCCGGGTGCC	Human read 2 primer
HS RJ2-4	162820C10	TTCAGGTCCTCCAGCACTGAGAGCCGGGTCCC	Human read 2 primer
HS RJ2-5	162820C12	TTCAGGTCCTCGAGCACCAGGAGCCGCGTGCC	Human read 2 primer
HS RJ2-6	162820C09	TTCAGGTCCTCCAGCACGGTCAGCCTGCTGCC	Human read 2 primer
HS RJ2-7	162820C11	TTCAGGTCCTCTGTGACCGTGAGCCTGGTGCC	Human read 2 primer